Achievable Data Rate Improvement Analysis of a THz Multiple RIS-Assisted Factory System Based on Ray Tracing

Higo T. P. da Silva, Ruan D. Gomes, Hugerles S. Silva,
Felipe A. P. de Figueiredo, **Rausley A. A. de Souza**[1]

[1]National Institute of Telecommunications
Inatel, Brazil

Dezember 18, 2024

ICSPCS 2024

Introduction

- The technical objectives of **Industry 5.0** fundamentally depend on developing of **ultra-low latency and reliable communication** (uLLRC) and **ultra-high data rate** (uHDR) services based on 6G technologies
- Among the main advances envisioned for 6G, the use of **ultra-wide bandwidth** in the terahertz (THz) bands is particularly notable
- This frequency band (**100 GHz–10 THz**) provides **tens of GHz of available bandwidth**, making it suitable for **applications with high data rates**, such as those required by **uHDR**

Introduction

- Another innovative 6G approach is the application of reflective intelligent surfaces (RISs) in industrial settings
- These surfaces **provide control over electromagnetic scattering**, significantly **improving coverage** in environments with a high likelihood of signal obstruction

- The effective implementation of **6G industrial networks** fundamentally depends on accurately characterizing the wireless communication channel
- Ray tracing emerges as a powerful method capable of describing the **nature of electromagnetic propagation** in the THz band, including particular **phenomena of high frequencies**, such as **diffuse scattering**

Objectives and Contributions

- This study aims to investigate the **performance gain** provided by **multiple RISs**
    - **Multiple-input single-output** (MISO) system operating in the **140 GHz**
    - **Indoor factory** (InF) environment
- This investigation is conducted through computational **ray tracing simulations** based on the **shooting-and-bouncing rays** (SBR) method
- The performance of the simulated systems is evaluated based on the achievable data rate (ADR) and compared to that of an equivalent non-RIS-assisted system

System Model

- **Access point** (AP) equipped with a **uniform linear array** (ULA) of N antenna elements that communicates with a **single-antenna receiver** (RX)
- The link between the AP and the receiver is determined by the **direct channel (DC)**, composed by line-of-sight (LoS) and scattered rays

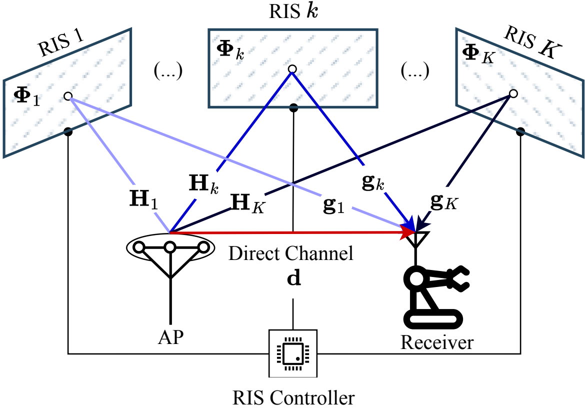

System Model

- The **communication is assisted by K RISs**, in which each surface contains M **reflecting elements**
- A cascaded channel is formed by the **AP-RIS and RIS-RX paths**, defining the **RIS-assisted channels** (RACs)
- The **phases of the passive elements** of the RISs can be **adjusted by the controller** to **appropriately modify the scattering** of the incident wave

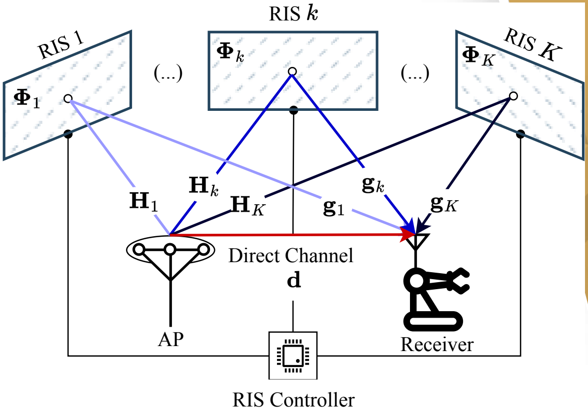

System Model

- It is assumed that each RIS element and the receiving points are in the **far-field zone of the AP**
- The **receiver is in the near-field zone** of the RISs

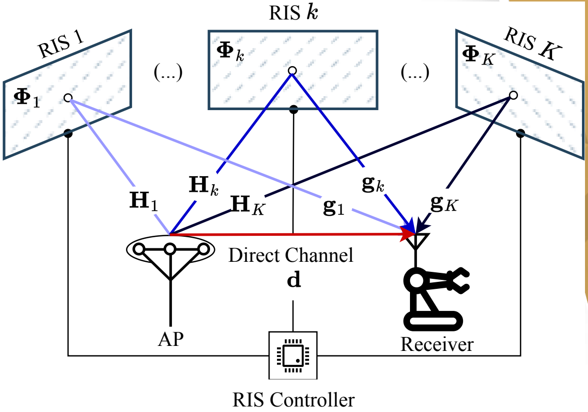

RIS Scattering Modeling

Channel Coefficients

$$h_{k,m} = \sqrt{\frac{\rho_{\text{a};k,m} A_{\text{el;k}} G_{\text{el}}(\bar{\mathbf{r}}_{k,m}, \mathbf{n}_k)}{4\pi \ell_{k,m}^2}} e^{-j\frac{2\pi}{\lambda}\ell_{k,m}}$$

$$g_{k,m} = \sqrt{\frac{\bar{\rho}_{\text{a};k,m} A_{\text{RX}} G_{\text{el}}(\bar{\mathbf{s}}_{k,m}, \mathbf{n}_k)}{4\pi l_{k,m}^2}} e^{-j\frac{2\pi}{\lambda}l_{k,m}}$$

$\rho_{\text{a};k,m}$ and $\bar{\rho}_{\text{a};k,m}$ are the atmospheric molecular absorption factors in the incidence and scattering paths, $G_{\text{el}}(\cdot,\cdot)$ is the reflecting element radiation pattern, $A_{\text{RX}} = \lambda^2/4\pi$ is the receiver antenna aperture.

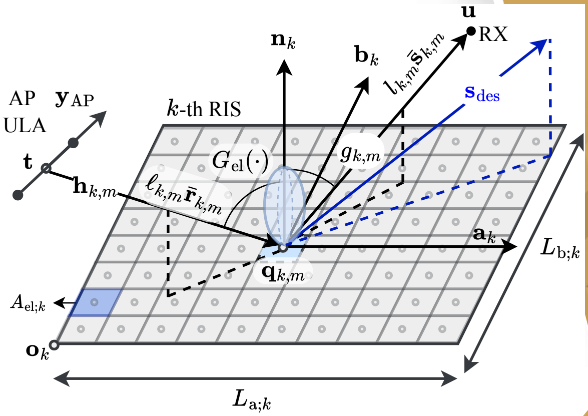

Performance Analysis

- Assuming **perfect knowledge of the channels**, the AP applies a **maximum ratio combining (MRC) precoding** to design the vector $\mathbf{w}$

RIS Phases Design

$$\Phi_{k,m} = [\boldsymbol{\phi}_k]_m = \exp\left(-\angle[\mathbf{z}_k]_m\right), \tag{1}$$

in which $\mathbf{z}_k = \mathbf{V}_k \mathbf{d}^\star \in \mathbb{C}^{M\times 1}$

Achievable Data Rate

$$R = \log_2\left(1 + \frac{P}{\sigma_\mathsf{n}^2}\left\|\sum_{k=1}^{K} \alpha_k \boldsymbol{\phi}_k^T \mathbf{V}_k + \mathbf{d}^T\right\|^2\right), \tag{2}$$

Ray Tracing Modeling

- Applying the **SBR method**, the ray tracing algorithm comprises three primary stages:
  - **Transmission**: multiple rays are emitted along the angular sphere from a designated source point.
  - **Tracing**: the rays' lengths are gradually increased and it is evaluated whether the rays interact with objects in the environment
  - **Reception**: virtual spheres are defined around the receiver points. Rays that intercept these reception spheres contribute to the channel impulse response (CIR) of the corresponding link
- The **ray tracing model** considers the following effects:
  - **Specular reflection**
  - **Diffraction** (Uniform Theory of Diffraction – UTD)
  - **Diffuse scattering** (Beckmann-Kirchoff theory)
  - **Atmospheric molecular absorption** (ITU-R P.676)

Ray Tracing Modeling

Normalized Ray Power – Direct Channel

$$p_{\mathrm{r}} = \frac{\lambda^2}{(4\pi)^2} A_{\mathrm{fs}} \rho_{\mathrm{t}} \prod_i \left(A_{\mathrm{re}} \Gamma_i^2 \rho_{\mathrm{ds};i}^2 \right) \prod_j \left(A_{\mathrm{d};j} D_j^2 \right) \prod_k \left(A_{\mathrm{ds};j} \zeta_k^2 \right) . \tag{3}$$

- A_{fs} is the free-space divergence factor
- $\rho_{\mathrm{t}} = \rho_{\mathrm{p}} \rho_{\mathrm{a}}$, in which ρ_{p} is the polarization mismatch loss and ρ_{a} is the atmospheric molecular absorption attenuation
- Γ_i and D_j are the reflection and diffraction losses
- ζ_k is the diffuse scattering loss
- A_{re}, A_{d}, and A_{ds} are the divergence factors related to the reflection, diffraction, and diffuse scattering, respectively

Propagation Environment Characterization

- Real industrial warehouse located in the **technological hub of the Federal Institute of Paraíba** (IFPB) in **João Pessoa, Brazil**
- An **area** of 8.3 m × 18.35 m, with a **ceiling height** of 3 m
- The warehouse is enclosed by **concrete** and **plaster walls**, each with a thickness of 0.2 m, and features **glass windows**

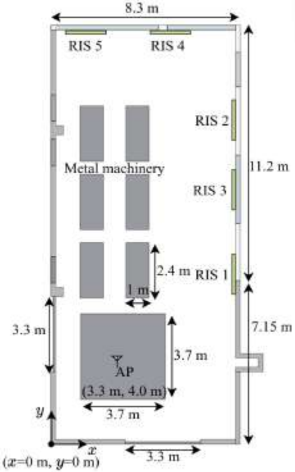

Propagation Environment Characterization

- The space contains various **machines and equipment**, represented as **metal blocks** with a **height of 1.8 m**
- **Five RISs**, with dimensions of 2 m$\times$1 m ($A_{\text{RIS;k}} = 2$ m^2), are distributed along the environment

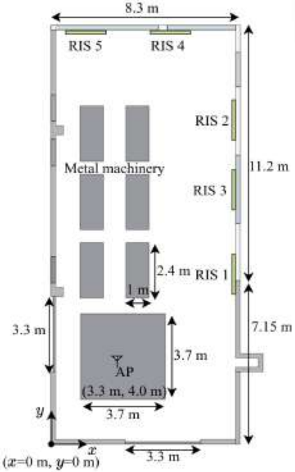

Simulation Results

- Five simulation cases are considered. For each case, the **number of active RISs varies**. In the k-th simulation case, denoted as C$_k$, with $k \leq 5$; the RISs with indices in the set $S_k = \{1, \cdots, k\}$ are activated

Table 1: Specifications of ray tracing simulations.

Parameter	**Value**
AP coordinates	(4.0 m, 3.3 m)
AP height – h_{AP}	3.0 m
Number of antenna elements – N	32
Receiver height – h_{rx}	1.5 m
Carrier frequency	140 GHz
Transmitted power – P	0 dBm
Noise variance – σ_{n}	-94 dBm
Angular resolution – $\Delta\theta$	0.067°
Maximum number of reflections	6
RIS elements directivity gain – G_0	8 (9 dBi)
RIS elements reflection losses – α_k	0.8

Simulation Results

Figure 1: Map of LoS conditions related to the AP position obtained from ray tracing simulations.

Simulation Results

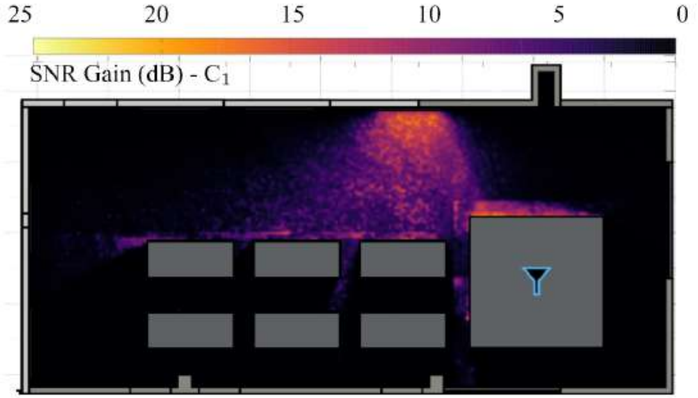

Figure 2: Heat map of the point-to-point SNR gain provided by the RIS for the simulation case C_1 considering $M = 100$.

Simulation Results

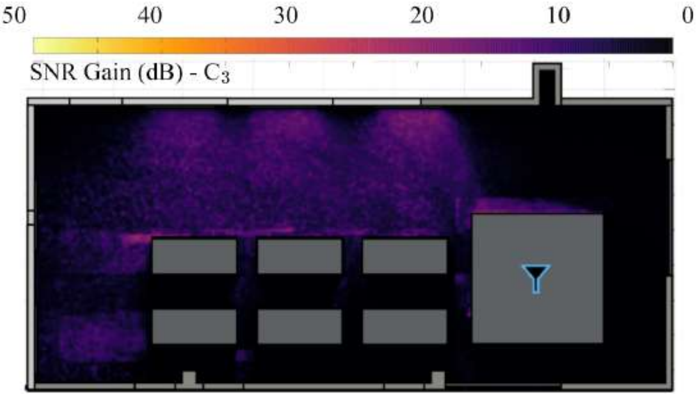

Figure 3: Heat map of the point-to-point SNR gain provided by the RISs for the simulation case C_3 considering $M = 100$.

Simulation Results

Table 2: Summary of the ray tracing simulations results.

M	**Link Type**	**Achievable Rate (bit/s/Hz)**				
		C_1	C_2	C_3	C_4	C_5
100	Global	4.04	4.40	4.63	5.23	5.83
	LoS	4.44	4.81	5.07	5.45	6.06
	NLoS	2.61	2.95	3.08	4.43	5.01
1000	Global	4.70	5.55	5.93	6.85	7.69
	LoS	5.10	5.94	6.37	6.99	7.88
	NLoS	3.24	4.15	4.39	6.36	7.05

Non-RIS-assisted system, Average ADRs of 3.59 bit/s/Hz (global), 3.98 bit/s/Hz (LoS), and 2.21 bit/s/Hz (NLoS).

Simulation Results

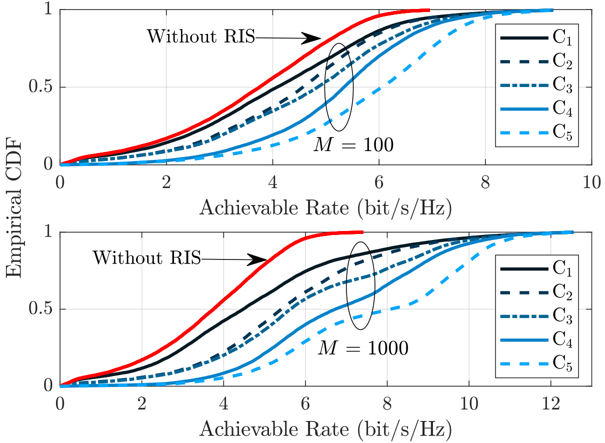

Figure 4: Empirical CDF curves of the ADR obtained from the ray tracing simulations considering $M \in \{100, 1000\}$.

Simulation Results

Numerical Approximation of the Average ADR as a Function of M

$$\hat{R}_{\text{avg}}(M) = \mu_1 M^{\mu_2} + \tilde{R}_{\text{avg};0}, \tag{4}$$

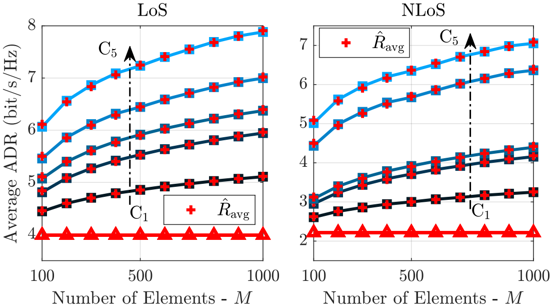

Figure 5: Curves of average ADR values as a function of the number of elements M for the considered simulation cases.

Conclusions

- The results have shown that deploying **five RISs** with **100 elements** each achieves an **average data rate of 6.06 bit/s/Hz**, an **increase of 2.08 bit/s/Hz** compared to a system without RISs.
- The **gain in the average** rate is **more significant in non-line-of-sight (NLoS) links**
- With **four RISs of 1000 elements each**, there has been a **187% improvement in the average ADR of NLoS links**
- A **power expression** enabled the **numerical characterization of the average ADR's variation rate** concerning the number of RIS elements
- These findings demonstrate that **applying RISs in InF environments effectively enhances performance and standardizes coverage**, particularly in **THz band applications**

Thanks

The authors thank CNPq (305536/2021-4), FAPESQ, PPGEE/IFPB, and the IFPB Innovation Hub. This work was partially supported by CNPq (Grant References 311470/2021-1 and 403827/2021-3), by the projects XGM-AFCCT-2024-2-5-1, XGM-FCRH-2024-2-1-1, and XGM-AFCCT-2024-9-1-1 supported by xGMobile – EMBRAPII-Inatel Competence Center on 5G and 6G Networks, with financial resources from the PPI IoT/Manufatura 4.0 from MCTI grant number 052/2023, signed with EMBRAPII, by RNP, with resources from MCTIC, Grant No. 01245.020548/2021-07, under the Brazil 6G project of the Radiocommunication Reference Center (Centro de Referência em Radiocomunicações - CRR) of the National Institute of Telecommunications (Instituto Nacional de Telecomunicações - Inatel), Brazil, and by Fapemig (PPE-00124-23, APQ-04523-23, APQ-05305-23 and APQ-03162-24).